Efficiency of Filtering Materials Used in Respiratory Protective Devices Against Nanoparticles

Agnieszka Brochocka
Krzysztof Makowski
Katarzyna Majchrzycka

Central Institute for Labour Protection – National Research Institute (CIOP-PIB), Łódź, Poland

Piotr Grzybowski

Faculty of Chemical and Process Engineering, Warsaw University of Technology, Warsaw, Poland

The basic aim of this research was to establish the efficiency of filtering materials widely used in respiratory protection devices with particular interest in their porosity, degree of electric and changeable process parameters, such as the flow rate of the test nanoaerosol and the size range of nanoparticles. Tests were carried out with an NaCl solid aerosol of 3.2×10^5 particles/cm³ for the range of particle size of 7–270 nm, at aerosol flow rate of 1800, 2700, 3600, 4500 and 5400 L/h. The tests showed that electrospun nonwovens were the most effective filtering materials for nanoparticles over 20 nm. Melt-blown electret nonwovens with lower porosity than electrospun nonwovens had higher values of penetration of 1%–4%. Those materials provided very efficient protection against nanoparticles of certain sizes only.

efficiency   filtering material   nanoparticles   respiratory protective devices

1. INTRODUCTION

Nanotechnology is a rapidly developing field of research because nanoscale objects can be used in most human activities. Numerous tests are carried out to develop nanomaterials with a range of specific properties not present in the same materials in macroscale. This increasing interest in nanomaterials has resulted in many new ways they can be produced. This development is also connected with new threats facing both the environment and human health [1].

Currently, nanoparticles pose danger in many areas: metallurgy (powders and welded smoke, powders created in the process of precise cutting and sanding); electronics and environmental protection (carbon nanotubes); printing, chemical and paper industries (titanium dioxide nanoparticles, self-cleaning surfaces, SiO_2-Ag); textile industry (silver nanoparticles, SiO_2-Ag) and cosmetic industry (SiO_2-Ag, nanocapsules) [2, 3, 4, 5, 6]. In the near future, as the use of nanomaterials increases, so will the number of workers exposed to them.

Research aimed at estimating the risk posed by inhaling nanoparticles proved that their number and their surface play a vital role in workers' pneumonia [1, 7, 8, 9]. Tests on nanoquartz and titanium dioxide showed that the toxicity of certain types of nanoparticles may be connected with

the reactivity of their surface. As the size of a particle decreases, the number of atoms on its surface increases significantly in relation to the number of atoms inside the particle. This creates particles with increased reactivity; they are a more effective catalyst for various processes. As a result, modifications on the surface of a particle result in a layer that is harmful for a person exposed to the inhalation of nanoparticles.

Therefore, it is important to study ways of evaluating risk posed by the development of nanotechnology and to improve collective and personal protection. Most nanoparticles penetrate into the human body through the respiratory system. If safe production processes are not possible or there are contraindications for collective protection, it is necessary to use personal respiratory protective devices (RPDs). It is important to select ones that efficiently separate nanoparticles from the air stream.

Currently, there are no European standards, harmonized with Directive 89/686/EEC [10], on evaluating the efficiency of RPDs against aerosols with nanoparticles. Therefore, there is no information on whether or not RPDs available in the European Union can efficiently protect workers exposed to the inhalation of nanoparticles at their workplace.

The present study was undertaken to establish the efficiency of filtering materials commonly used in RPDs, with particular focus on their porosity, degree of charge and changeable process parameters, such as the flow rate of the test nanoaerosol and the size of the nanoparticles.

Theory

Aerosol nanoparticles are deposited on filter fibres as a result of diffusion, electrostatic effect, direct interception and internal deposition. All these mechanisms contribute to the total filtering efficiency, which depends on particle diameter, flow rate, fibre diameter, packing density and electric charges both on fibres and particles. Equations 1–2 describe single fibre efficiency due to diffusion [1]:

$$E_D = 2 \cdot Pe^{-2/3}, \tag{1}$$

$$Pe = d_f U_0 / D, \tag{2}$$

where E_D = single fibre efficiency, Pe = Peclet number, d_f = fibre diameter, U_0 = air velocity, D = particle diffusion coefficient. Equation 3 is

$$E_R = \frac{1}{2Ku} \left[2(1+R) \cdot \ln(1+R) \right. \\ \left. - (1+R) + \frac{1}{(1+R)} \right], \tag{3}$$

where E_R = direct interception deposition, Ku = Kuwabara number, R = interception parameter. For the filter packing density α, $Ku = -\ln(\alpha)/2 - 3/4 + \alpha - \alpha^2/4$ and $R = d_p/d_f$, where Ku = Kuwabara number, R = interception parameter, d_p = particle diameter, d_f = fibre diameter. Internal deposition, even though it is not high for nanoparticles, can be calculated with Equation 4:

$$E_I = \frac{J \cdot Stk}{2 \cdot Ku^2}, \tag{4}$$

where E_I = internal deposition, Stk = Stoke's number $Stk = \rho_p d_p^2 C_c U_0 / (18 \mu d_f)$, ρ_p = particle density, d_p = particle diameter, C_c = Cunningham slip correction, U_0 = gas velocity, μ = gas viscosity, d_f = fibre diameter. Electrostatic interactions between charged particles and charged fibres enhance particle deposition. Equation 5 describes the electrostatic force F_E acting between the particle and the fibre:

$$F_E = \frac{2Qq}{r} = \frac{2\pi (d_f/2)^2 \lambda_e q}{r}, \tag{5}$$

where Q = fibre charge, q = particle charge, d_f = fibre diameter, λ_e = fibre charge density, r = distance between particle and fibre. Within the flow in Stoke's regime, Equation 6 gives the dimensionless parameter of the electrostatic deposition N_{Qq}:

$$N_{Qq} = \frac{4Qq}{3\pi\mu d_p C_c \, d_f U_0}, \tag{6}$$

where Q = fibre charge, q = particle charge, μ = gas viscosity, d_p = particle diameter, C_c = Cunningham slip correction, d_f = fibre diameter, U_0 = gas velocity.

Natanson's Equation 7 expresses the single fibre efficiency E_{Qq} for a charged particle and a charged fibre:

$$E_{Qq} = \pi N_{Qq}, \qquad (7)$$

where N_{Qq} = electrostatic deposition.

In this paper, the electrostatic effect on particle deposition was calculated according to Pitch [11]. The single fibre efficiency E_{Qq} is related to the direct interception deposition E_R:

$$E_{Qq} = y_F \cdot E_R, \qquad (8)$$

where $y_F = x_F \left(\pi - ar\cos(x_F) \right) + \left(1 - x_F^2 \right)^{\frac{1}{2}}$ for $x_F \leq 1$,

$y_F = \pi x_F$ for $x_F \geq 1$

and $x_F = \dfrac{2 |\lambda_e \cdot q| B}{\dfrac{d_f}{2} U_0 E_R}$, $B = \dfrac{1}{6\pi\mu\left(\dfrac{d_p}{2}\right)C_c}$,

where λ_e = fibre charge density, q = particle charge, d_f = fibre diameter, U_0 = gas velocity, E_R = direct interception deposition.

Shaw described all these deposition mechanisms [11]. It is possible to calculate separately their contribution in the overall penetration P of the filtering material of the thickness L and the total filtering efficiency of a single fibre E. Single fibre efficiency is a sum of these for all mechanisms considered ($E = \sum E_i$):

$$P = \exp\left(-\frac{4E\alpha L}{\pi d_f (1-\alpha)} \right), \qquad (9)$$

where P = overall penetration, E = filtering efficiency of a single fibre, α = filter packing density, L = thickness of filtering material, d_f = fibre diameter.

To compare the filtering properties of various nonwoven filtering materials, the measurements took place in the same conditions in a special filter holder with the same test aerosol. The aerosol of nanoparticles initially passed through a chamber with a Kr_{85} source, where it was neutralized and gained equilibrium charge with the charge distribution $f(n_p)$ described with Boltzmann equilibrium:

$$f\left(n_p\right) = \frac{\left[-\dfrac{\left(n_p e\right)^2}{d_p kT} \right]}{\sum\limits_{-\infty}^{+\infty}\left[-\dfrac{\left(n_p e\right)^2}{d_p kT} \right]}, \qquad (10)$$

where $f(n_p)$ = charge distribution, e = elementary charge, d_p = size of particle carrying n_p elementary units of charge, k = Boltzman constant, T = absolute temperature. Within this test aerosol, in the range of diameters of 7.1–269.0 nm, there were particles of the same electric mobility, with a single charge only.

The filtering efficiency for small particles is relatively high due to the strong diffusion effect but any further possible increase in the deposition of these particles is desirable because they are very harmful. New types of commercial filtering materials were used in the experimental study on the filtering efficiency of solid nanoparticles. One of the filtering materials was a melt-blown non-woven prepared from polypropylene in CIOP-PIB's laboratory. In this case, the fibres were charged to enhance the expected electrostatic effect and filtering efficiency.

2. EXPERIMENTAL

2.1. Tested Materials

Table 1 lists the most common filtering materials used in RPDs, which were selected for the tests.

Fibre diameter was measured with a scanning electric microscope. Surface electric charge was measured with a frequency modulation (FM) electrostatic field gauge to determine low-frequency electric fields from –2000 to 2000 kV/m. The surface electric charge of nonwovens was measured in nine evenly spread points on samples of 0.04 m². Air flow pressure drops were established for the air flow of 3600 L/h.

2.2. Test Method

The values of nanoaerosol penetration for filtering materials were established by measuring the number of particles of a test aerosol in front of and behind the filter sample. Filter samples of

TABLE 1. Characteristics of Nonwoven Filtering Materials

Type of Nonwoven	Material	Fibre Diameter (µm)	Surface Mass (g/m^2)	Material Density (g/cm^3)
Needle-punched nonwoven	PE	18.5	160	0.930
Nonwoven with triboelectric effect	PAN/PP	21.0	150	0.806
Melt-blown nonwoven with corona charging	PP	1.3	86	0.900
Electrospun nonwoven (from polymer solution)	styrene copolymer	1.6	45	0.900

Type of Nonwoven	Thickness (mm)	Filter Packing Density (–)	Medium Electrostatic Charge of 10^{-9}C/0.15 m^2	Fibre Charge (C/m)
Needle-punched nonwoven	4.0	0.043	+2.3	$3.59 \cdot 10^{-15}$
Nonwoven with triboelectric effect	3.8	0.049	−27.6	$-5.1 \cdot 10^{-14}$
Melt-blown nonwoven with corona charging	2.1	0.045	−47.1	$-6.5 \cdot 10^{-16}$
Electrospun nonwoven (from polymer solution)	0.6	0.083	+4.6	$1.85 \cdot 10^{-16}$

Notes. PE = polyethylene, PP = polypropylene, PAN = polyacrylonitryle.

0.01 m^2 were placed in the filter holder. A test aerosol of solid NaCl nanoparticles was generated by nebulizing a 0.1% water solution of NaCl with a Collinson atomizer (model 3076 from TSI, USA). The aerosol then passed through a dryer with a dessicant before it reached the test chamber with a Kr_{85} source, where it was neutralized. Its concentration was 3.2×10^5 particles/cm^3. The measuring range of the setup made it possible to test particles of 7–270 nm, divided into 90 ranges of diameter.

Each test of each sample at a given air flow rate took 7 min: three cycles, 126 s each and 15-s breaks between the cycles. The average penetration was calculated for the three cycles. Tests were carried out at five aerosol flow rates: 1800, 2700, 3600, 4500 and 5400 L/h. The surface of the tested samples was the same in all measurements, 0.01 m^2. Climatic conditions during the tests were ambient temperature of 20 ± 5 °C and relative air humidity of 50% ± 20%. Figure 1 is a diagram of the test stand.

The average diameter of aerosol particles was 78 nm (Figure 2). Upstream and downstream aerosol samples passed an electrostatic classifier of particle size (No. 6 in Figure 1). Aerosol concentration was measured with a condensation nanoparticle counter (No. 7 in Figure 1). The data were recorded and stored.

3. RESULTS AND ANALYSIS

The values of the penetration for aerosol particles in the range of 7.1–269.0 nm were calculated on the basis of the measurements and theoretically. Figures 3–11 present the results: they average values for 10 samples of each nonwoven filtering material.

3.1. Nanoparticle Penetration for a Needle-Punched Nonwoven

Figures 3–4 show the results of the measured penetration of the test aerosol depending on particle diameter for different flow rates. There was a difference between the needle-punched nonwoven (Figure 3) and the nonwoven with the triboelectric effect (Figure 4). In the former, penetration reached 80% for particles of 100–270 nm, whereas in the latter, for the same range of diameter, the maximum value of penetration was under 20%. This proves that for almost the same structure of the filtering material, a significant improvement of efficiency against nanoparticles is possible when the electrostatic effect of attraction between a fibre and depositing nanoparticle is induced [12]. Unfortunately, this effect is not observed in the smallest particles of 7–25 nm, when penetration for both types of stitched nonwovens approaches 100%. The lines in Figures 3–4
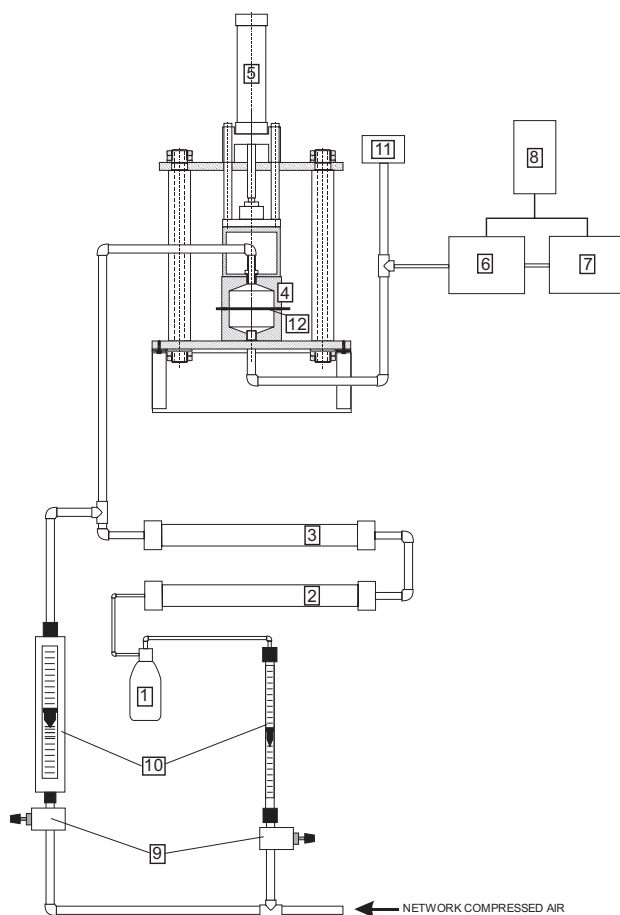
Figure 1. Diagram of experimental setup. *Notes.* 1 = nanoaerosol generator, 2 = desiccant, 3 = electrostatic charge neutralizer, 4 = testing chamber, 5 = sample holder, 6 = electrostatic classifier of particle size, 7 = condensation nanoparticle counter, 8 = personal computer, 9 = compressed air valves, 10 = flow meters, 11 = high-efficiency filter, 12 = test sample.
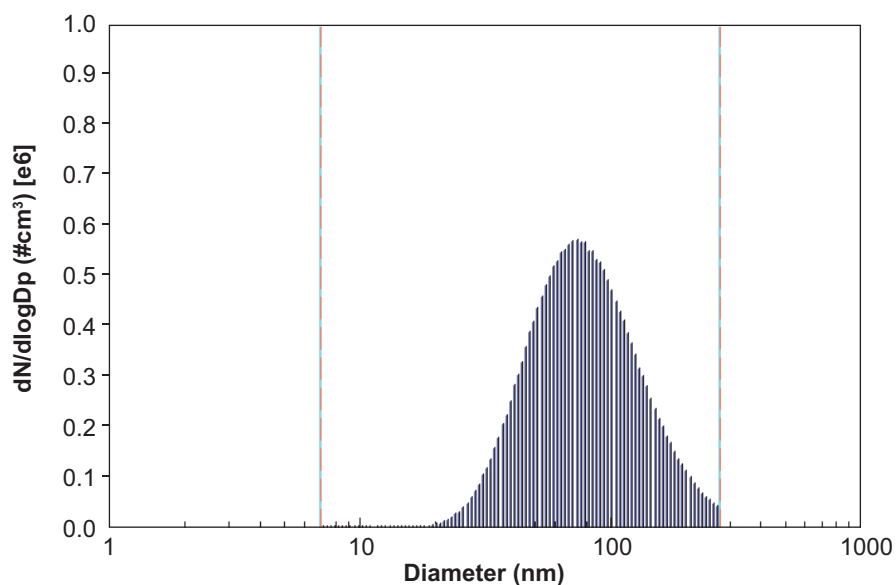
**Figure 2. Size spread of aerosol with NaCl particles.**

denote theoretical calculations of penetration; they show general and expected tendencies of changes in penetration values. Changing the parameters of the filtering materials in the theoretical calculations leads to a better fit only in the case of the needle-punched nonwoven (Figure 3), not the nonwoven with the triboelectric effect (Figure 4). This may be caused by a nonuniform charge distribution on fibres and repulsion of some fraction of the particles.

There was a significant difference in filtering efficiency for both variants of nonwovens in the range of 25–100 nm. Together with an increase in nanoparticle diameter for the needle-punched nonwoven, there was also an increase in penetration, whereas there was a rapid decrease for the nonwoven with the triboelectric effect. It was also assumed that for the nonwoven with the triboelectric effect, there was a visible increase in nanoparticle deposition due to the electrostatic effect. The higher the value of aerosol flow, the greater the value of penetration both in calculations and in experiments. There was no such regularity for the needle-punched nonwoven.
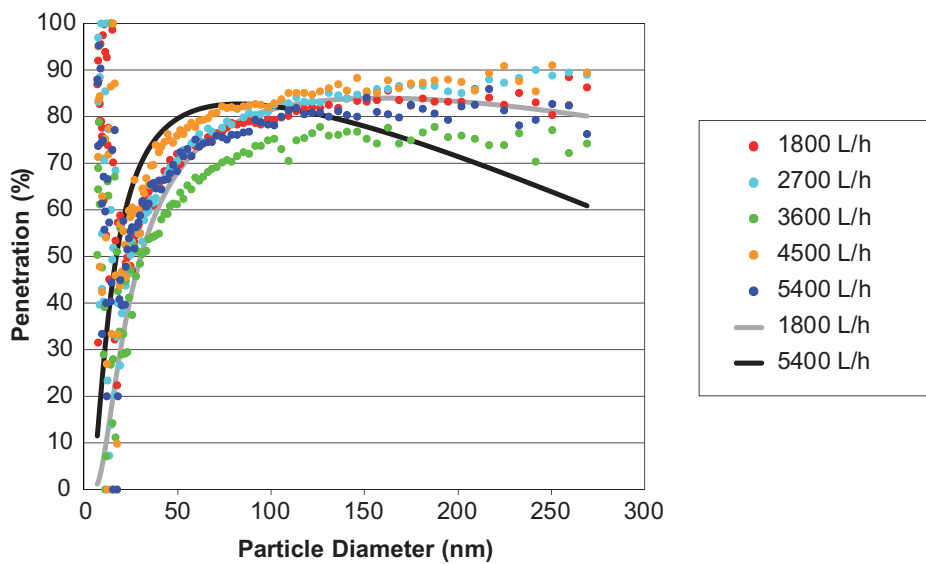
Figure 3. Effect of particle diameter on penetration of a nanoaerosol with NaCl particles for a needle-punched nonwoven at different aerosol flow rates. *Notes.* Lines denote calculated values.
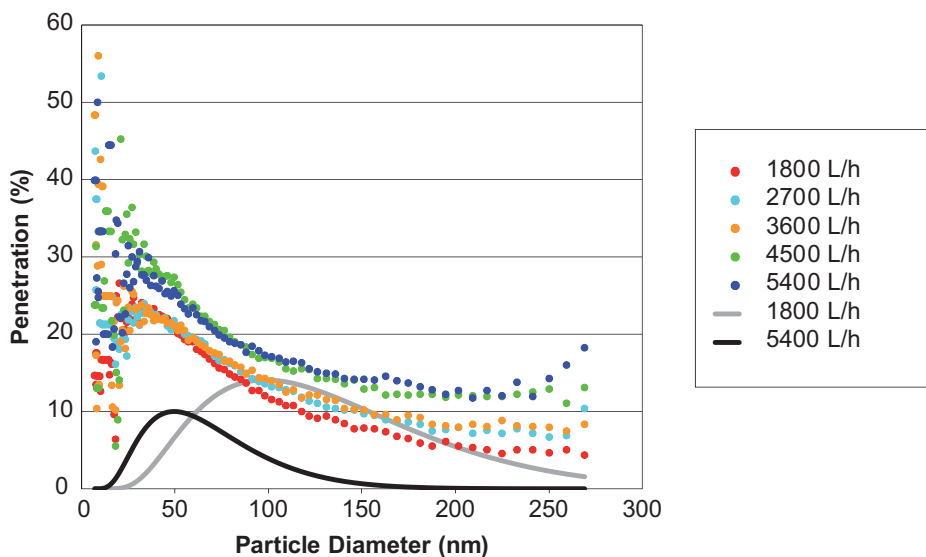
Figure 4. Effect of particle diameter on penetration of a nanoaerosol with NaCl particles for a nonwoven with triboelectric effect at different aerosol flow rates. *Notes.* Lines denote calculated values.

3.2. Nanoparticle Penetration for a Melt-Blown Electret Nonwoven

Figure 5 shows measured values of penetration for melt-blown nonwovens, activated in the field of corona discharge [13]. In this case, there was a clear dependency between penetration and aerosol flow rate. The values of nanoparticle penetration followed the increase in aerosol flow rates. For melt-blown nonwovens, the penetration for particles ranging from 2 to 25 nm reached the maximum value of 4%. For particles ranging from 25 to 75 nm, penetration increased from 1.50% to 3.5%, depending on the aerosol flow rate. For greater sizes of nanoparticles, there was a decrease in penetration. Theoretically calculated penetration had values close to 0%; they are not shown in Figure 5. Penetration was calculated theoretically for $\alpha = 0.01$; see lines 1800 and 5400 L/h in Figure 5. Those lines show increased values of penetration for smaller particles for a greater flow rate. This was expected and experimental data confirmed this. Penetration values measured for greater particles (i.e., particles over 100 nm) are not in step with theoretical considerations. Increased nonuniformity of fibre spreading within the sample structure and the presence of channels explains this.

3.3. Nanoparticle Penetration for an Electrospun Nonwoven

Figure 6 presents values of penetration measured in tests of samples of an electrospun nonwoven filtering material. There was a clear dependence of penetration on the flow rate of test nanoaerosols. Higher flow rates corresponded with an increase in penetration values. For the electrospun nonwoven, there was full deposition of nanoparticles of up to 20 nm (there was no penetration). For particles ranging from 20 to 70 nm, the penetration values increased up to 0.2%–0.9%, depending on the flow rate. For greater nanoparticles, there was a further gradual decrease in penetration. Figure 6 shows the theoretically calculated penetration, which reached 0.25%–1.6%. If the theoretically calculated values of penetration were to be in the range of the measured ones (0.6%), the fibre diameter would need to be 0.4 µm, whereas it was 1.6 µm. This indicates the role of a very strong electrostatic effect in the filtration process inside this filtering structure and a wider range of the fibre diameter inside the filter sample.
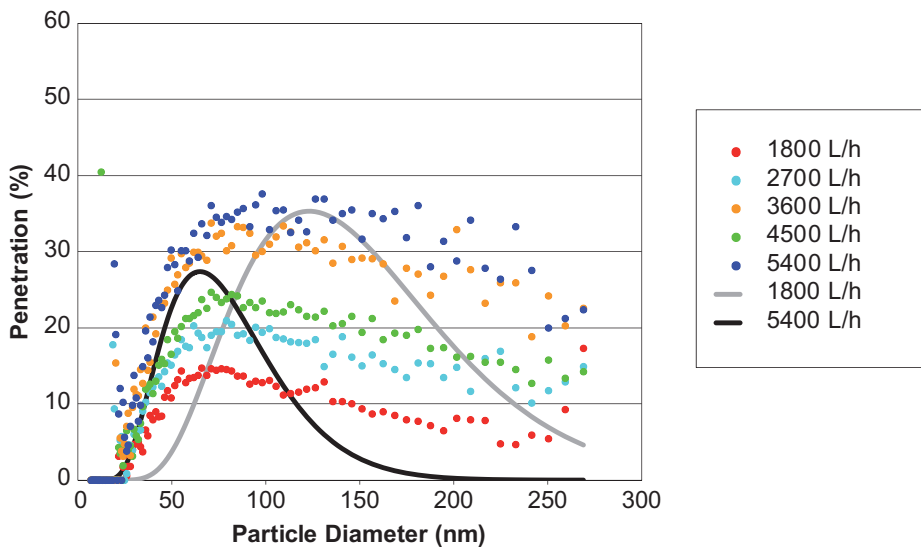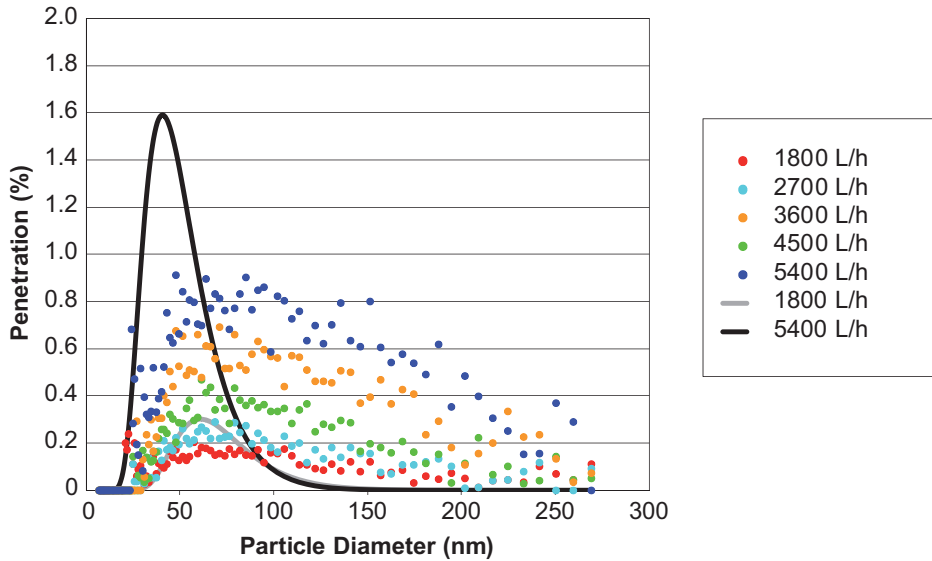

Figure 5. Effect of particle diameter on penetration of a nanoaerosol with NaCl particles for a melt-blown nonwoven at different aerosol flow rates. *Notes.* Lines denote calculated values.
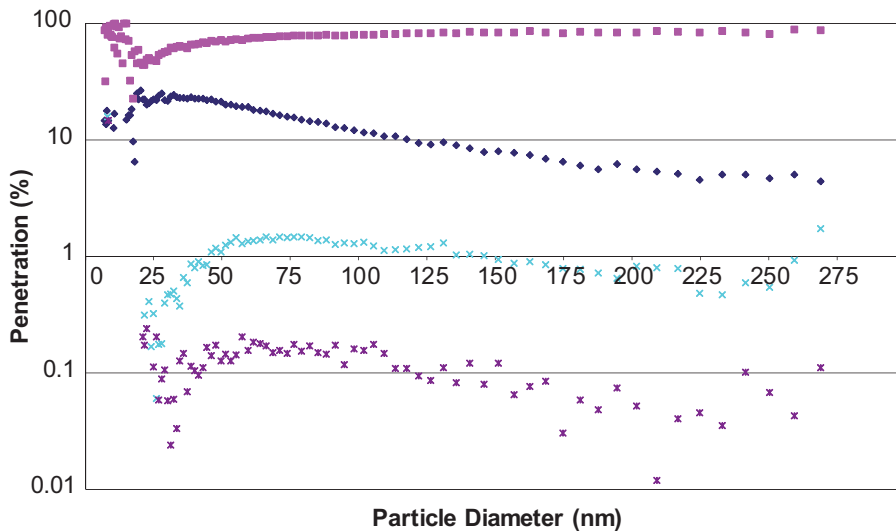
Figure 6. Effect of particle diameter on penetration of a nanoaerosol with NaCl particles for an electrospun nonwoven at different aerosol flow rates. *Notes.* Lines denote calculated values.

3.4. Comparison

Figure 7–11 show the overall results of penetration for all filtering materials by nanoaerosol flow rate.

The tests showed that the electrospun nonwoven with fine fibres and high porosity was the most effective filtering material for all particle diameters. An electret nonwoven with a penetration value of 1%–4% is a melt-blown nonwoven with lower porosity than an electrospun nonwoven.

It is difficult to draw conclusions on a single way of improving the efficiency of filtering materials to stop nanoparticles. As for the whole range of sizes among nanoparticles, neither porosity nor introducing the effects of electrostatic powers of attraction between nanoparticles and fibres provides acceptable results [12, 13]. It is thus necessary to search for technologies of modelling and creating filtering nanostructures, which previous studies have already indicated [14, 15, 16].

Figure 7. Effect of particle diameter on penetration of a nanoaerosol with NaCl particles for filtering materials at aerosol flow rate of 1800 L/h. *Notes.* ◆ = nonwoven with tribolectric effect, ■ = needle-punched nonwoven, × = melt-blown nonwoven, × = electrospun nonwoven.
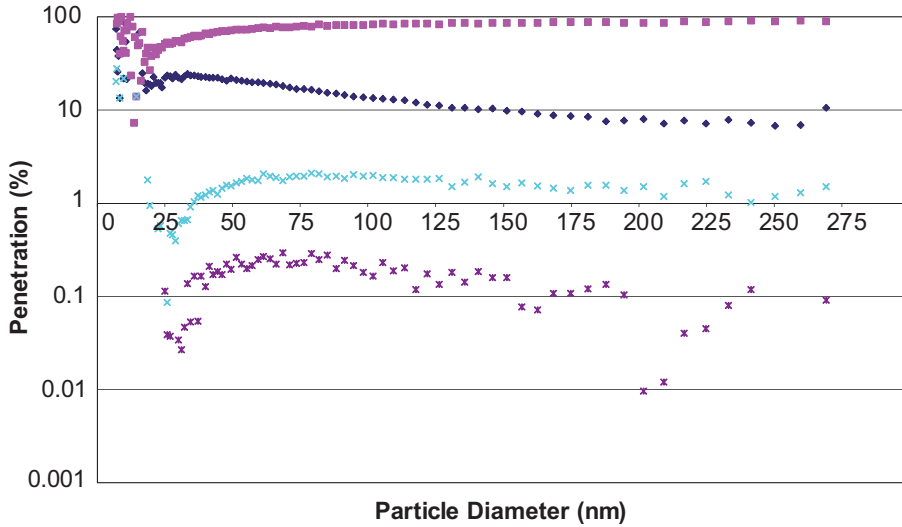
Figure 8. Effect of particle diameter on penetration of a nanoaerosol with NaCl particles for filtering materials at aerosol flow rate of 2700 L/h. *Notes.* ◆ = nonwoven with tribolectric effect, ■ = needle-punched nonwoven, × = melt-blown nonwoven, × = electrospun nonwoven.
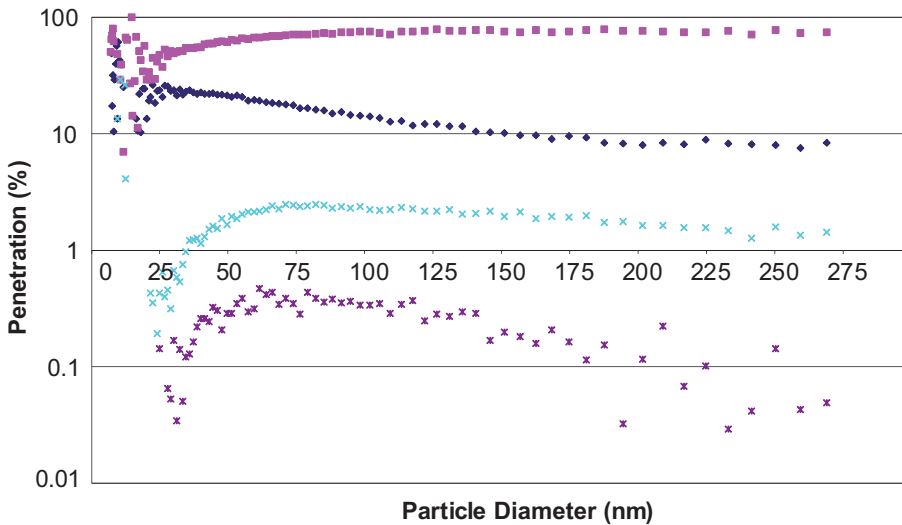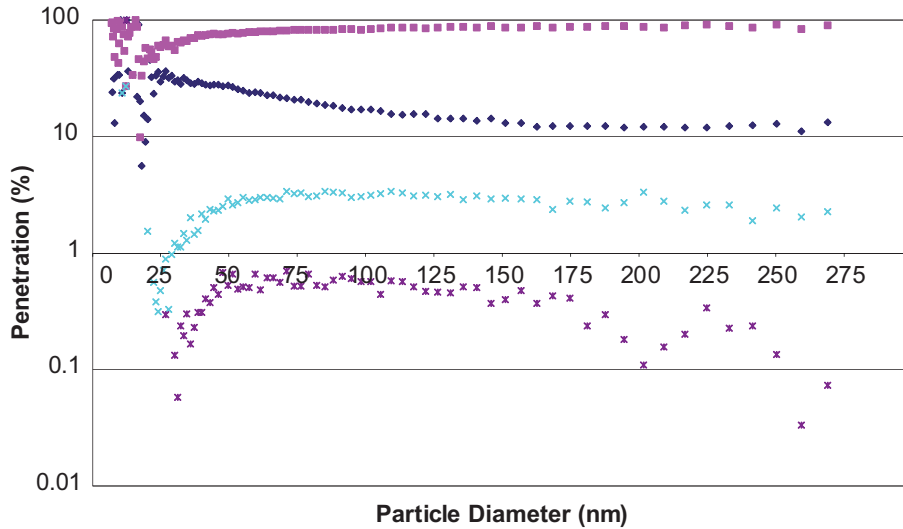

Figure 9. Effect of particle diameter on penetration of a nanoaerosol with NaCl particles for filtering materials at aerosol flow rate of 3600 L/h. *Notes.* ◆ = nonwoven with tribolectric effect, ■ = needle-punched nonwoven, × = melt-blown nonwoven, × = electrospun nonwoven.

4. SUMMARY AND CONCLUSIONS

The experiments showed that the efficiency of filtering aerosol nanoparticles by the nonwovens commonly used in RPDs depends on the size range of the nanoparticles of the harmful aerosol, on the one hand, and, on the other, on the characteristics of the fibrous structure of the filtering materials and their electrostatic features. It is important that nonwoven filtering materials with great porosity and a relatively low value of air flow resistance should not be used in constructing RPDs against nanoparticles. Even using the triboelectric effect in these materials might not sufficiently improve their efficiency. Moreover, the purpose of these filtering materials does not seem

Figure 10. Effect of particle diameter on penetration of a nanoaerosol with NaCl particles for filtering materials at aerosol flow rate of 4500 L/h. *Notes.* ◆ = nonwoven with tribolectric effect, ■ = needle-punched nonwoven, × = melt-blown nonwoven, ✕ = electrospun nonwoven.
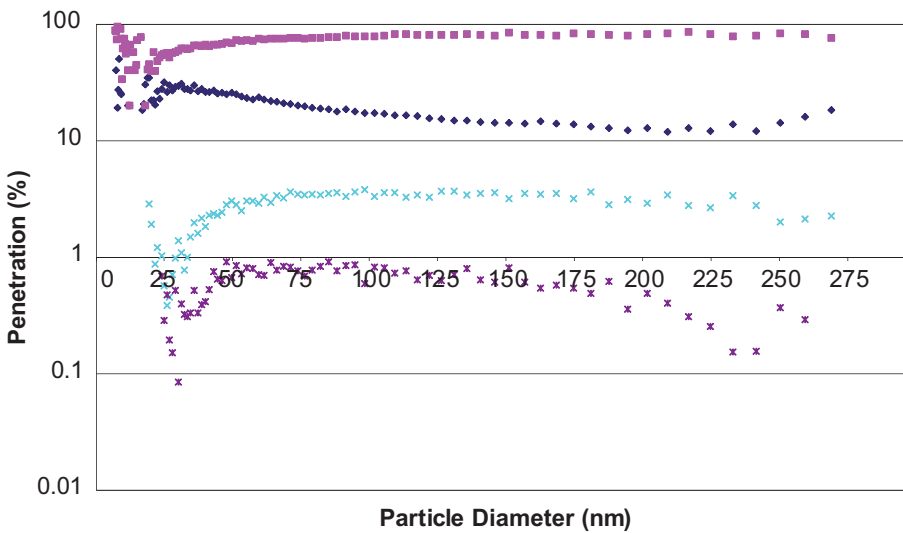
Figure 11. Effect of particle diameter on penetration of a nanoaerosol with NaCl particles for filtering materials at aerosol flow rate of 5400 L/h. *Notes.* ◆ = nonwoven with tribolectric effect, ■ = needle-punched nonwoven, × = melt-blown nonwoven, ✕ = electrospun nonwoven.

to justify using them to improve the loading capacity in the case of nanoaerosols. This seems relatively unimportant, considering the small sizes of the particles and the low values of nanoaerosol concentration compared to the concentration of powders, mists or smokes in real industrial conditions.

Referring to the analysis of more porous materials with the pressure drop of 140–950 Pa, it is important that these types of materials are not used now in RPDs that meet the expectations for efficient filtering of nanoparticles. The tests point out that it is hard to find RPDs with systems of filtering materials that ensure capturing nanoparticles from the whole spectrum of diameters, i.e., 7–270 nm. The materials tested now are highly efficient in some ranges of particle diameters only.

It is necessary to continue research on innovative filtering materials or systems of such materials that would ensure efficient protection for workers exposed to inhalation of harmful aerosols with nanoparticles.

REFERENCES

1. Grass RN, Limbach LK, Athanassiou EK, Stark WJ. Exposure of aerosols and nanoparticle dispersions to in vitro cell cultures: a review on the dose relevance of size, mass, surface and concentration. J Aerosol Sci. 2010;41(12):1123–42.

2. Sinha N, Ma J, Yeow JT. Carbon nanotube-based sensors. J Nanosci Nanotechnol. 2006;6(3):573–90.

3. Mao S, Lu G, Chen J. Carbon-nanotube-assisted transmission electron microscopy characterization of aerosol nanoparticles. Aerosol Science. 2009;40(2):180–4.

4. Park J, Kwak BK, Bae E, Lee J, Kim Y, Choi K, et al. Characterization of exposure to silver nanoparticles in a manufacturing facility. J Nanopart Res. 2009;11(7):1705–12.

5. Boddu SR, Gutti VR, Ghosh TK, Tompson RV, Loyalka SK. Gold, silver and palladium nanoparticle/nano-agglomerate generation, collection, and characterization. J Nanopart Res. 2011;13(12):6591–601.

6. Reijnders L. The release of TiO_2 and SiO_2 nanoparticles from nanocomposites. Polym Degrad Stab. 2009;94(5):873–6.

7. Warheit DB, Sayes CM, Reed KL, Swain KA. Health effects related to nanoparticle exposures: environmental, health and safety considerations for assessing hazards and risks. Pharmacol Ther. 2008;120(1):35–42.

8. Friedrichs S, Schulte J. Environmental, health and safety aspects of nanotechnology implications for the R&D in (small) companies. Science and Technology of Advanced Materials. 2007;8(1–2):12–8.

9. Kandlikar M, Ramachandran G, Maynard A, Murdock B, Toscano WA. Health risk assessment for nanoparticles: a case for using expert judgment. Nanotechnology and Occupational Health. 2007;9:137–56.

10. Council Directive 89/686/EEC of 21 December 1989 on the approximation of the laws of the Member States relating to personal protective equipment. OJ. 1989; L399:18–38. Retrieved April 2, 2013, from: http://eur-lex.europa.eu/LexUriServ/LexUriServ.do?uri=CONSLEG:1989L0686:20031120:en:PDF.

11. Shaw DT. Fundamentals of aerosol science. New York, NY, USA: Wiley; 1978.

12. Brochocka A, Ruszkowski K. Some aspects of manufacturing electret nonwoven filters by a conventional method with utilisation of the triboelectric effect. Fibres and Textiles in Eastern Europe. 2000;(3):69–72.

13. Brochocka A. Characteristics of melt-blown filter materials produced by simultaneous blowing of polymer melt from two extruders. Fibres and Textiles in Eastern Europe. 2001;(4):66–9.

14. Przekop R, Gradoń L. Deposition and filtration of nanoparticles in the composites of nano- and microsized fibres. Aerosol Sci Technol. 2008;42(6):483–93.

15. Gradoń L, Podgórski A, Bałazy A. Filtration of nanoparticles in the nanofibrous filters. In: FILTECH EUROPA 2005. Conference Proceedings. 2005. Vol. II, p. 178–85.

16. Podgórski A, Bałazy A, Gradoń L. Application of nanofibers to improve the filtration efficiency of the most penetrating aerosol particles in fibrous filters. Chem Eng Sci. 61(12):6804–15.